Crack growth from internal defects and related size-effect in VHCF

Available online at www.sciencedirect.com

ScienceDirect

Procedia Structural Integrity 5 (2017) 247–254

Structural Integrity Procedia

www.elsevier.com/locate/procedia

2nd International Conference on Structural Integrity, ICSI 2017, 4-7 September 2017, Funchal, Madeira, Portugal

Crack growth from internal defects and related size-effect in VHCF

Davide S. Paolino[a]*, Andrea Tridello[a], Giorgio Chiandussi[a], Massimo Rossetto[a]

[a]*Politecnico di Torino, Department of Mechanical and Aerospace Engineering, Corso Duca degli Abruzzi 24, Turin 10129, Italy*

Abstract

It is well-known in the literature that fatigue cracks in VHCF originate from small internal defects. More than 95% of the total VHCF life is consumed in originating the so-called Fine Granular Area (FGA) around the small initial defect. Within the FGA, crack growth takes place even if the Stress Intensity Factor (SIF) is smaller than the threshold value for crack growth. Researchers proposed different explanations for this unexpected phenomenon but they unanimously accept that a weakening mechanism occurs around the initial defect, which permits crack growth below the SIF threshold.
In the present paper, crack growth in the VHCF regime is innovatively modeled and a general expression for the fatigue limit is then obtained. The statistical distribution of the fatigue limit is also defined and a model for the fatigue limit as a function of the risk-volume is proposed. Finally, the proposed model is successfully applied to an experimental dataset.

Peer-review under responsibility of the Scientific Committee of ICSI 2017

Keywords: Design and Structural Assessment; Fracture Analysis

1. Introduction

Due to the increased fatigue life requested to components for structural applications, the research on the Very-High-Cycle Fatigue (VHCF) behavior of materials has recently gained significant attention. Fatigue cracks in the VHCF regime generally originate from internal material defects: inclusions, pores, voids or microstructural inhomogeneities.

* Corresponding author. Tel.: +39-011-090-5746; fax: +39-011-090-6999.
E-mail address: davide.paolino@polito.it

2452-3216
Peer-review under responsibility of the Scientific Committee of ICSI 2017
10.1016/j.prostr.2017.07.124

In the VHCF regime, fracture surfaces typically exhibit the well-known fish-eye morphology, with the so-called Fine Granular Area (FGA) around the initial internal defect (Sakai et al., 2002). The FGA plays a key role in the VHCF response, since more than 95% of the total life is consumed in its origination. The average crack growth rate within the FGA is extremely small and, unexpectedly, crack can grow even if the Stress Intensity Factor (SIF) is smaller than the threshold value for crack growth. To justify this particular behavior, a number of micromechanical models have been proposed in the VHCF literature (see, e.g., the review by Li et al., 2016). Regardless of the specific micromechanical model, it is generally acknowledged that a weakening mechanism occurs around the initial defect, thus permitting the crack growth below the SIF threshold. In Paolino et al. (2017), the Authors proposed and experimentally validated a model for crack growth from the initial defect in the VHCF regime. The model can be effectively used for a quantitative description of the different weakening mechanisms proposed in the literature and permits to define a general expression for the fatigue limit.

In the present paper, the model is generalized in a statistical framework. The statistical distribution of the fatigue limit is analytically defined. Size-effects on the fatigue limit distribution are also modeled starting from the well-known dependency between the internal defect size and the loaded volume of material (risk-volume). An illustrative numerical example, based on experimental data, is finally reported in order to show the applicability of the proposed model.

Nomenclature

FGA	Fine Granular Area
SIF	Stress Intensity Factor
rv	random variable
LEV	Largest Extreme Value distribution
HV	Vickers Hardness
a_c, a_d, $a_{d,0}$, a_{FGA}, a_{FiE}	projected areas of defects
$c_{th,g}$, $\alpha_{th,g}$, $c_{th,r}$, $\alpha_{th,r}$	parameters involved in SIF thresholds
c_I, m_I, c_{II}, m_{II}, c_{III}, m_{III}, c_s, m_s	Paris' constants in the three stages of crack growth
k_d	SIF of defect
$k_{th,g}$, $k_{th,l}$, $k_{th,r}$	SIF thresholds, deterministic value
N_f	number of cycles to failure
N_I, N_{II}, N_{III}	number of cycles in the three stages of crack growth
$F_{\sqrt{A_{d,0}},V}$	Cumulative distribution function of the LEV
$f_{\sqrt{A_{d,0}},V}$	Probability density function of the LEV
V, V_{exp}	risk-volumes
$s_{l,\sqrt{a_{d,0}},\alpha}$	Conditional logarithm of the fatigue limit rv
z_α	quantile of a standardized Normal cdf
$F_{S_l\|\sqrt{a_{d,0}}}$	cdf of the conditional fatigue limit
$\mu_{\sqrt{A}}$, $\sigma_{\sqrt{A}}$, $\sigma_{lK_{th,g}}$	Parameters of statistical distributions

2. Methods

In Section 2.1, a general expression for modeling the crack growth rate from the initial defect up to the VHCF failure is presented. In Section 2.2, the statistical distribution of the defect size and the related size-effects are analyzed and discussed. Finally, in Section 2.3, the statistical distribution of the fatigue limit is analytically defined and a model for the fatigue limit as a function of the risk-volume is proposed.

In the following, according to Paolino et al. (2017), $k_{th,g}$ denotes the global SIF threshold, $k_{th,r}$ denotes the reduction SIF, k_d denotes the SIF for an internal defect, $k_{th,l}$ denotes the local SIF threshold (i.e., $k_{th,l} = k_{th,g} - k_{th,r}$), $a_{d,0}$ is the projected area of the initial defect and a_{FGA} is the projected area of the FGA.

2.1. Crack growth rate within the FGA

In the VHCF literature (Tanaka and Akiniwa, 2002; Marines-Garcia et al., 2008; Su et al., 2017), the crack growth rate within the FGA is commonly modeled with the Paris' law. Three stages can be present in the crack growth rate diagram related to a VHCF failure from internal defect (Fig. 1):

- Stage I: the below-threshold region within the FGA, from $k_{d,0}$ (SIF associated to the initial defect) up to $k_{th,g}$;
- Stage II: the steady stage, from the border of the FGA (SIF equal to $k_{th,g}$) up to the border of the fish-eye (with SIF equal to k_{FiE});
- Stage III: the unsteady stage, beyond the fish-eye border (with SIF larger than k_{FiE}, up to the failure).

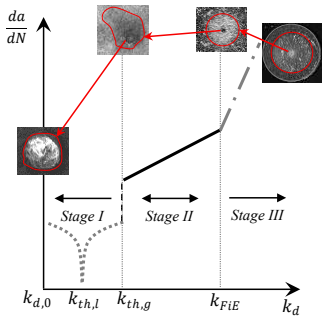

Fig. 1. The three stages of crack propagation in a crack growth rate diagram for VHCF failures from internal defects.

For a stress ratio equal to -1, the modified Paris' law proposed by Donahue et al. (1972) is considered to model the crack growth within the FGA:

$$\frac{da}{dN} = c_I\left(k_d - k_{th,l}\right)^{m_I}, \tag{1}$$

where c_I and m_I are the Paris' constants related to Stage I, from the initial defect size $\sqrt{a_{d,0}}$ up to $\sqrt{a_{FGA}}$.

According to (Tanaka and Akiniwa, 2002; Marines-Garcia et al., 2008; Su et al., 2017), in Stage II, from the border of the FGA up to the border of the fish-eye (with size $\sqrt{a_{FiE}}$), the crack growth rate follows the conventional Paris' law:

$$\frac{da}{dN} = c_{II}k_d^{m_{II}}, \tag{2}$$

where c_{II} and m_{II} are the two Paris' constants related to Stage II, from $\sqrt{a_{FGA,max}}$ up to $\sqrt{a_{FiE}}$.

Generally, crack propagates beyond the fish-eye border until it reaches the border of the final fracture, with size $\sqrt{a_c}$. In these cases, a third stage of crack propagation is visible on the fracture surfaces and it can be modeled again with the conventional Paris' law (Su et al., 2017):

$$\frac{da}{dN} = c_{III}k_d^{m_{III}}, \tag{3}$$

where c_{III} and m_{III} are the two Paris' constants related to Stage III, from $\sqrt{a_{FiE}}$ up to $\sqrt{a_c}$. It is worth to note that, if the final fracture occurs when the crack size reaches the border of the fish-eye, Stage III can be neglected.

The number of cycles to failure, N_f, can be expressed as the sum of the number of cycles consumed within the three stages of propagation:

$$N_f = N_I + N_{II} + N_{III}. \tag{4}$$

Following the VHCF literature (see, e.g., Su et al., 2017), N_I can be estimated by subtracting, from the experimental N_f, the numbers of cycles consumed in Stages II and III, which are obtained through integration of Eqs. (2) and (3), respectively.

According to Paolino et al., (2017), the experimental N_I values ($N_{I,exp}$) can be used for the estimation of the Paris' constants c_I, m_I and of the parameters $c_{th,r}$ and $\alpha_{th,r}$ involved in the expression of the $k_{th,l}$. Parameter estimates are obtained through the nonlinear Least Squares Method by minimizing the sum of squared percent errors between the experimental $\log_{10}(N_{I,exp})$ values and the estimated $\log_{10}(N_{I,est})$ values computed through integration of Eq. (1). Finally, an estimate of the fatigue limit can be defined, according to the procedure described in Paolino et al., (2017).

2.2. Statistical distribution of the initial defect size and related size-effect

Size-effects significantly affect the VHCF response of materials (Furuya, 2011; Tridello et al., 2015): the larger the risk-volume (volume of material subjected to a stress larger than the 90% of the maximum stress), the larger the probability of large defects, with a subsequent reduction of the VHCF strength. The dependency between the fatigue limit and the risk-volume is generally modeled by taking into account the statistical distribution of the internal defect size. According to the VHCF literature (Murakami, 2002), the defect originating failure can be considered as the largest defect present within the specimen risk-volume and, therefore, in a statistical framework the internal defect size random variable (rv) follows a Largest Extreme Value (LEV) distribution.

The cumulative distribution function (cdf) of the LEV distribution is reported in Eq. (5): it provides the probability of an internal defect with size smaller than $\sqrt{a_{d,0}}$ in a volume V larger than the risk-volume of the tested specimens (V_{exp}).

$$F_{\sqrt{A_{d,0}},V} = \left\{\exp\left[-\exp\left(-\frac{\sqrt{a_{d,0}}-\mu_{\sqrt{A}}}{\sigma_{\sqrt{A}}}\right)\right]\right\}^{\frac{V}{V_{exp}}}, \tag{5}$$

where $\mu_{\sqrt{A}}$ and $\sigma_{\sqrt{A}}$ are the two constant parameters of the distribution. The probability density function (pdf) of the LEV distribution, $f_{\sqrt{A_{d,0}},V}$, is expressed by:

$$f_{\sqrt{A_{d,0}},V} = \frac{V}{V_{exp}} \cdot \left(F_{\sqrt{A_{d,0}},V_{exp}}\right)^{\frac{V}{V_{exp}}-1} \cdot f_{\sqrt{A_{d,0}},V_{exp}}. \tag{6}$$

According to Murakami, (2002), the parameters of the LEV distribution can be estimated from the defect sizes $\sqrt{a_{d,0}}$ measured on the fracture surfaces of the tested specimens (i.e., with $V = V_{exp}$ in Eqs. (5) and (6)).

2.3. Statistical distribution of the fatigue limit and related size-effect

The statistical distribution of the fatigue limit is here defined. According to Paolino et al., (2016) the α-th quantile of the fatigue limit for a given defect size can be expressed as:

$$s_{l,\sqrt{a_{d,0}},\alpha} = c_{th,g} \frac{c_{s_l}(HV+120)}{\sqrt{a_{d,0}}^{1/2-\alpha_{th,g}}} \cdot 10^{z_\alpha \cdot \sigma_{K_{th,g}}}, \quad (7)$$

where z_α denotes the α-quantile of a standardized Normal cdf, $c_{th,g}$, $\alpha_{th,g}$ and $\sigma_{K_{th,g}}$ are the parameters involved in the statistical distribution of the global SIF threshold (Paolino et al., 2016; Paolino et al., 2017), HV is the Vickers hardness of the material and $c_{s_l} = \left(\frac{(1/2-\alpha_{th,g})0.5\sqrt{\pi}}{(\alpha_{th,g}-\alpha_{th,r})c_{th,r}}\right)^{\frac{1/2-\alpha_{th,g}}{1/2-\alpha_{th,r}}} \frac{\alpha_{th,g}-\alpha_{th,r}}{0.5\sqrt{\pi}(1/2-\alpha_{th,r})}$.

The α-th quantile of the fatigue limit as a function of the risk-volume can be obtained from the definition of marginal cdf and by taking into account the defect size distribution:

$$\alpha = \int_0^\infty F_{S_l|\sqrt{a_{d,0}}}\left(s_l;\sqrt{a_{d,0}}\right) \cdot f_{\sqrt{A_{d,0}},V}\left(\sqrt{a_{d,0}};V\right) \cdot d\sqrt{a_{d,0}}, \quad (8)$$

where $F_{S_l|\sqrt{a_{d,0}}}$ denotes the cdf of the fatigue limit for a given defect size. For a given risk-volume V, the α-th quantile of the fatigue limit can be obtained by solving Eq. (8) with respect to s_l.

3. Application to an experimental dataset

The models proposed in Section 2 are here applied to an experimental dataset. VHCF tests are carried out on Gaussian specimens (Tridello et al., 2015) made of an AISI H13 steel with Vickers hardness 560 kg_f/mm^2 and $V_{exp} = 2300$ mm^3. Details on the testing setup and on the tested material are reported in Tridello et al. (2015) and in Tridello et al. (2016) and they will not be recalled here for the sake of brevity. Twelve specimens are loaded at constant stress amplitude up to failure. The number of cycles to failure ranges from $4.2 \cdot 10^7$ to $3.85 \cdot 10^9$ cycles. The initial defect sizes ($\sqrt{a_{d0}}$) and the FGA sizes ($\sqrt{a_{FGA}}$) are measured from pictures taken by a Scanning Electron Microscope (SEM) and by an optical microscope. In order to take into account the stress variation within the V_{exp}, the local stress amplitude in the vicinity of the initial defect is considered as the stress amplitude applied during the test. The local stress amplitudes are in the range 500 ÷ 635 MPa.

The parameters $c_{th,g}$, $\alpha_{th,g}$ and $\sigma_{K_{th,g}}$ involved in the fatigue limit expression (Eq. 7) are estimated from the FGA sizes and the $k_{th,g}$ values by using the Least Squares Method (Paolino et al., 2017). Fig. 2 shows the $k_{th,g}$ values with respect to $\sqrt{a_{FGA}}$ together with the estimated model. The 0.1-th and the 0.9-th quantiles are also depicted.

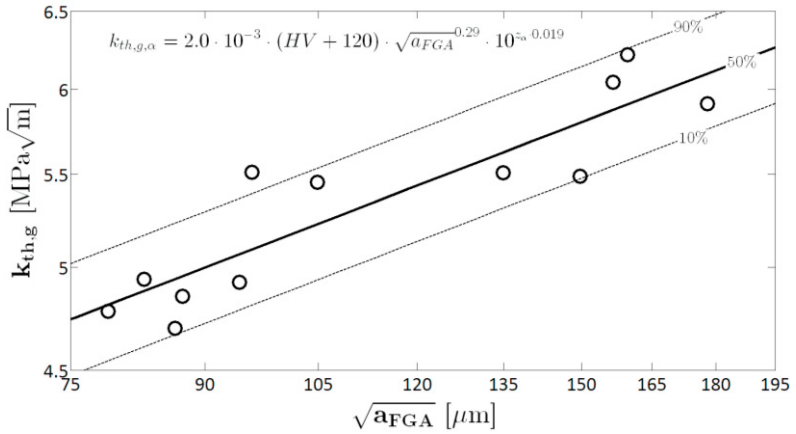

Fig. 2. Global SIF threshold variation as a function of the FGA size.

As shown in Fig. 2, the assumed linear model is in good agreement with the experimental data (11 failures out of 12 are inside the 80% confidence interval).

The parameters c_I, m_I, $c_{th,r}$ and $\alpha_{th,r}$ are estimated through the nonlinear Least Squares Method (Paolino et al., 2017). The fatigue limit for a given defect size is then estimated according to Eq. (7). Fig. 3 shows the median, the 0.1-th and the 0.9-th quantiles of fatigue limit as a function of the initial defect size.

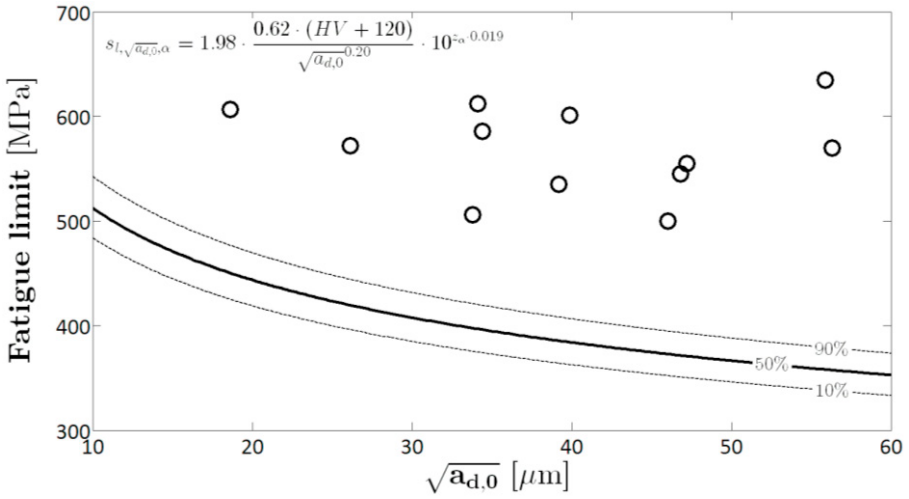

Fig. 3. Variation of the fatigue limit with the initial defect size.

According to Fig. 3, the fatigue limit decreases with the initial defect size (Murakami, 2002; Furuya, 2011). The estimated fatigue limit curves are below the experimental failures, as expected from the definition of fatigue limit. The proposed model is therefore effective in the estimation of the fatigue limit variation with respect to the initial defect size and ensures a reliable safety margin with respect to the experimental failures.

The distribution of initial defect size is estimated according to Murakami (2002). Fig. 4 shows the Gumbel plot of the $\sqrt{a_{d0}}$ together with the estimated LEV cdf. Parameter estimation is carried out by using the Maximum Likelihood Principle and by considering $V = V_{exp} = 2300$ mm^3.

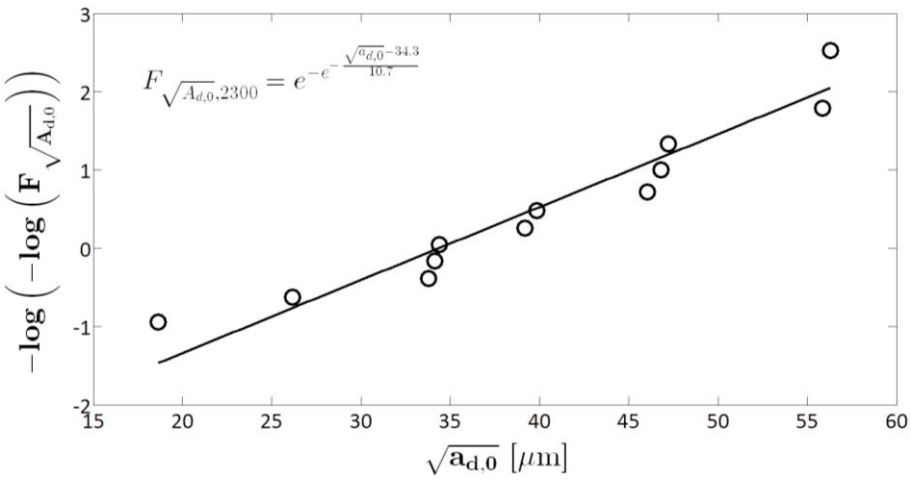

Fig. 4. Gumbel plot of the initial defect size for the investigated H13 steel.

From the initial defect size distribution and according to Eq. (8), the 0.1-th, 0.5-th and the 0.9-th quantiles of the fatigue limit are estimated for risk-volumes larger than V_{exp} and then depicted in Fig. 5.

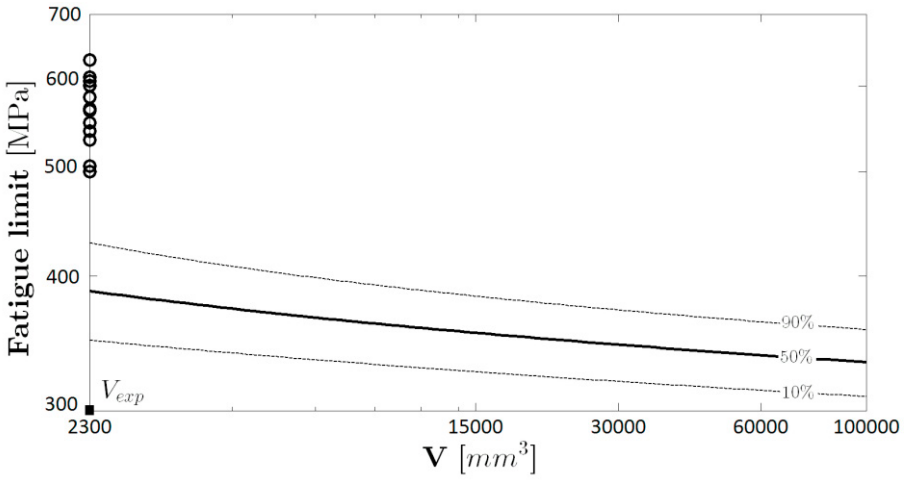

Fig. 5. Variation of the fatigue limit with the risk-volume.

As shown in Fig. 5, the proposed model is in good agreement with the experimental data: for a risk-volume V equal to V_{exp}, the fatigue limit curves are quite below the experimental failures. The proposed fatigue limit curves could be used for predicting the fatigue limit of components in service condition, characterized by risk-volumes significantly larger than the risk-volumes of the specimens commonly adopted in testing laboratories.

4. Conclusions

In the present paper, a general model for the fatigue limit is proposed. The statistical distribution of the fatigue limit for a given defect size and the fatigue limit variation with respect to the risk-volume are defined. The proposed model permits to take into account size-effects on the VHCF response and to predict the fatigue limit of components characterized by large risk-volumes.

The model was successfully applied to an experimental dataset. The fatigue limit curves as a function of the defect size and as a function of the risk-volume were estimated and were in agreement with the experimental data, since no failure occurred below the estimated fatigue limit curves.

The proposed model could be effectively adopted for the estimation of the fatigue limit curves when designing components subjected to VHCF.

References

Donahue, R. J., Clark, H. M., Atanmo, P., Kumble, R., McEvily, A. J., 1972. Crack opening displacement and the rate of fatigue crack growth. International Journal of Fracture Mechanics 8, 209-219.

Furuya, Y., 2011. Notable size effects on very high cycle fatigue properties of high-strength steel. Materials Science and Engineering: A 528, 5234-5240.

Li, Y. D., Zhang, L. L., Fei, Y. H., Liu, X. Y., Li, M. X., 2016. On the formation mechanisms of fine granular area (FGA) on the fracture surface for high strength steels in the VHCF regime. International Journal of Fatigue 82, 402-410.

Marines-Garcia, I., Paris, P. C., Tada, H., Bathias, C., Lados, D., 2008. Fatigue crack growth from small to large cracks on very high cycle fatigue with fish-eye failures. Engineering Fracture Mechanics 75, 1657-1665.

Murakami, Y., 2002. *Metal fatigue: effects of small defects and nonmetallic inclusions*. Elsevier, Oxford, UK.

Paolino, D. S., Tridello, A., Chiandussi, G., Rossetto, M., 2016. S-N curves in the very-high-cycle fatigue regime: statistical modeling based on the hydrogen embrittlement consideration. Fatigue & Fracture of Engineering Materials & Structures 39, 1319-1336.

Paolino, D. S., Tridello, A., Chiandussi, G., Rossetto, M., 2017. A general model for crack growth from initial defect in Very-High-Cycle Fatigue. Procedia Structural Engineering 3, 411-423.

Sakai, T., Sato, Y., Oguma, N., 2002. Characteristic S-N properties of high-carbon-chromium-bearing steel under axial loading in long-life fatigue. Fatigue & Fracture of Engineering Materials & Structures 25, 765-773.

Su, H., Liu, X., Sun, C., Hong, Y., 2017. Nanograin layer formation at crack initiation region for very-high-cycle fatigue of a Ti–6Al–4V alloy. Fatigue & Fracture of Engineering Materials & Structures 40, 979-993.

Tanaka, K., Akiniwa, Y., 2002. Fatigue crack propagation behaviour derived from S–N data in very high cycle regime. Fatigue & Fracture of Engineering Materials & Structures 25 775-784.

Tridello, A., Paolino, D. S., Chiandussi, G., Rossetto, M., 2015. VHCF response of AISI H13 steel: assessment of size effects through Gaussian specimens. Procedia Engineering 109, 121-127.

Tridello, A., Paolino, D. S., Chiandussi, G., Rossetto, M., 2016. Different inclusion contents in H13 steel: Effects on VHCF response of Gaussian specimens. Key Engineering Materials 665, 49-52.